



Modeling and Robust Fractional Order Fuzzy Sliding Mode Two Time Scale Controller Design for Synchronous Generator of ACP1000 Nuclear Power Plant in LabVIEW

Arshad Habib Malik^{1*}, Feroza Arshad², and Aftab Ahmad Memon³

¹Department of Basic Training, Chashma Centre of Nuclear Training, Pakistan Atomic Energy Commission, Chashma, Pakistan

²Department of Information System Division, Karachi Nuclear Power Generating Station, Pakistan Atomic Energy Commission, Karachi, Pakistan

³Department of Telecommunication Engineering, Mehran University of Engineering and Technology, Jamshoro, Sindh, Pakistan

Abstract: A state-of-the-art higher-order model of a synchronous generator is developed for ACP1000 nuclear power plant in the present research. The model is transformed into state space form. The state space model is decomposed into the two-time-scale framework. Based on the dynamics of the synchronous generator, fast and slow states are identified. The reduced order slow model is identified by neglecting the fast dynamics. A closed-loop model is developed in the frequency domain incorporating coupled and decoupled dynamics as separate transfer functions. The closed-loop model is configured as input-output pairs and two controllers are synthesized using a hybrid fraction order proportional integral derivative sliding surface oriented adaptive fuzzy two-time-scale control algorithm. The simulation model is developed in the graphical programming environment LabVIEW. The open and closed loop dynamics of the synchronous generator is simulated and analyzed in frequency and time domain separately. The proposed closed-loop framework is robust in performance, results are accurate and stable well within robust performance bounds.

Keywords: Synchronous Generator, Fractional Order, Adaptive Fuzzy Logic, Sliding Mode Control, ACP-1000, Nuclear Power Plant, LabVIEW.

1. INTRODUCTION

The synchronous generator of the Advanced Chinese Pressurized Water Reactor (ACP1000) type nuclear power plant is addressed in the present study for modeling, model reduction, control design, analysis and simulation purposes in the LabVIEW environment. The theoretical modeling aspects of the synchronous generator are discussed by Ernesto *et al.* [1]. A real-time experimental facility for synchronous generator is developed and simulation is performed by Helmy *et al.* [2]. A detailed first principle model is developed and simulated by Brazovac *et al.* [3] for the synchronous generator. A large industrial model of a 500 MWe power plant is analyzed and a PI controller is designed for the synchronous generator by Daphadar *et al.*

[4]. A large industrial model of a 1000 MWe power plant is analyzed and the PI controller is designed for the synchronous generator by Fodor *et al.* [5]. Modeling and fault detection for the synchronous generator is performed by Karnavas *et al.* [6] in LabVIEW. The phase diagram and capacity curve for the synchronous generator is analyzed by Sardar *et al.* [7] in LabVIEW. Experimental parametric model estimation is performed in the LabVIEW environment by Szabo *et al.* [8]. A comprehensive model of a synchronous generator is developed and simulated in LabVIEW and its performance is compared with the model developed in MATLAB for a 1000 MWe power plant by Dume [9]. A synchronous generator model is synthesized in a two-time scale framework by Mahmoud [10]. Research is further explored in the area of artificial

intelligence. A fuzzy logic controller is designed for synchronous generators by Sumina *et al.* [11]. The nonlinear sliding mode controller is established for an analytical model of a synchronous generator by Chang and Wen [12]. A nonlinear fractional order controller is designed for synchronous generator by Asadollahi *et al.* [13]. Further research is addressed for a hybrid fuzzy logic and two-time scale controller design for a robot arm manipulator by Lin and Lewis [14]. An investigation is performed for hybrid fractional order sliding mode controller synthesis for permanent magnet type synchronous generator by Xiong *et al.* [15]. Research is further expanded for the study of adaptive fractional order sliding mode controller design for the permanent magnet-type synchronous generator by Aghazamani and Delavari [16]. A most modern algorithm is developed for adaptive fractional order sliding mode fuzzy logic switching controllers for uncertain dynamics of the nuclear reactor of ACP1000 nuclear power plant by Malik *et al.* [17].

In this research work, a novel non-integer hybrid approach is adopted using a state-of-the-art algorithm developed in a graphical programming environment LabVIEW. The proposed algorithm encompasses new fractional order proportional integral derivative sliding surface, intelligent adaptive fuzzy logic and continuous two-time-scale (FO-PIDSMC-AFL-TTS) framework for closed-loop dynamics of the synchronous generator of the most sophisticated third-generation ACP1000 nuclear power plant. The proposed framework is the novel algorithm which is designed for the first time in LabVIEW for the nuclear industry.

2. MATERIALS AND METHODS

2.1 Synchronous Generator

The generator is a directly driven, three-phase, 50 Hz, 1500 rpm, 4-pole synchronous generator with a Hydrogen-cooled stator core and rotor, and water-cooled stator coils. The generator auxiliary system comprises of sealing oil system, hydrogen and carbon dioxide control system and stator coil cooling water system. The generator is cooled by circulating hydrogen, which transfers heat to hydrogen-cooler. The cold gas is forced to the rotor ventilation channel by the fan, and through the ventilation hole to the stator core around. The

stator coil is cooled by water. Cooling water enters from one end of the coil and exits from the other end after absorbing heat. Rotor coils are cooled by the internal axial duct by gas which back to the air gap after absorption heat. The gas flows through the generator and returns to the hydrogen-cooler. The stator is made with an inner frame and outer frame construction.

The generator is equipped with four hydrogen coolers. During installation, the coolers will be lowered into the generator through openings at the top of the generator frame. The magnetic core consists of stacking together cold-rolled, sheet metal magnetic segments with high permeability and low specific losses. The rotor shaft is machined from single steel forging free from injurious flaws and defects. The rotor shaft is mechanically coupled to the turbine. Floating-type retaining rings prevent straining of coil insulation. The retaining rings are made from forged 18Mn18Cr non-magnetic material.

The seal oil system is a double-ring type sealing oil system, used to seal the hydrogen with the frame of the generator, forming a hydrogen seal at the junction of the generator shaft. The seal oil system provides sealing oil to the sealing rings of the generator to prevent the escape of hydrogen from the generator, but also to prevent the outside air and moisture into the generator. The seal oil system ensures the stability of the differential pressure between the generator gas pressure and the seal oil pressure. Hydrogen is the cooling medium of the generator. The hydrogen and carbon dioxide gas system provides means for safely putting hydrogen in or taking hydrogen out of the generator by using carbon dioxide as a scavenging medium to prevent the air and hydrogen mixture and maintaining the gas pressure in the generator at the desired value. Hydrogen and carbon dioxide gas are supplied from the gas storage system. For cooling the generator stator coil by using the cooling water, the heat produced by the generator stator coil is taken away by the circulating high-purity water flowing through the stator hollow conductor (stator cooling water). The circulating high-purity water is cooled by closed-cycle cooling water in a water-water heat exchanger. The stator cooling water system provides circulating high-purity demineralized water to the generator stator coil.

Brushless excitation is adopted for the generator. The system contains an exciter, pilot and AVR (Automatic Voltage Regulator). The AVR contains the voltage regulator function together with limiters and other control circuits. The voltage regulator controls the output voltage of a power converter. The resulting DC voltage is supplied through field suppression equipment to the exciter field.

2.2 Synchronous Generator Modeling

The large-scale industrial synchronous generator is an electro-mechanical system. Various parameters/symbols and variables used hereafter in the process of synchronous generator modelling are defined as follows:

α_i = Variable Fraction Orders
 D_t = Time Derivative
 ω_m = Rotor Mechanical Frequency
 ω_e = Electrical Frequency
 τ_e = Electrical Torque
 R = Diagonal Matrix of Winding Resistances
 L = Symmetric Inductance Matrix
 L_m = Mutual Inductance between
 J = Rotor Moment of Inertia
 I_d = Generator Current d-axis System
 I_q = Generator Current q-axis System
 I_f = Field Current
 V_q = q-axis Winding Voltage
 ε = Separation Parameter
 S = Sliding Surface
 K_p = Proportional Gain
 K_i = Integral Gain
 K_D = Derivative Gain
 K_{SMC} = SMC Gain
 $u(t)$ = Control Input Signal
 u^F = Fractional Order Control Signal
 F = Fractional
 FO = Fractional Order
 PID = Proportional Integral Derivative
 SMC = Sliding Mode Control
 $AFLC$ = Adaptive Fuzzy Logic Controller
 TTS = Two Time Scale
 V_1 = Reference Input 1
 V_2 = Reference Input 2
 Y_1 = Cross Coupled Controlled Output 1
 Y_2 = Cross Coupled Controlled Output 2
 G_{11} = Transfer Function of Paired Input 1 and Output 1

G_{12} = Transfer Function of Paired Input 1 and Output 2

G_{21} = Transfer Function of Paired Input 2 and Output 1

G_{22} = Transfer Function of Paired Input 2 and Output 2

Cx = Product of Output Matrix and State Vector

Du = Product of Direct Transmission Matrix and Control Input

Bu = Product of Input Matrix and Control Input

$X_f(t)$ = Fast State Vector

$X_s(t)$ = Slow State Vector

λ_d = Flux Linkage along d-axis

λ_q = Flux Linkage along q-axis

λ_{abf} = Three Phase Flux Linkages in Stationary Frame

N = Number of Turns

θ = Rotor Angle

T = Transpose of Matrix

If α_i are the variable fractional orders of time domain differential operators $D_t^{\alpha_i}$ then the electrical dynamics of the synchronous generator are computed by the two-phase stator model as [3]:

$$D_t^{\alpha_1} \lambda_{abf} = -RL(\theta)^{-1} \lambda_{abf} + V_{abf} \quad (1)$$

The electrical torque is computed as:

$$\tau_e = D_t^{\alpha_2} \left(\frac{1}{2} \lambda_{abf}^T L(\theta)^{-1} \lambda_{abf} \right) \quad (2)$$

The mechanical speed of the rotor is computed as:

$$D_t^{\alpha_3} \omega_m = \frac{1}{J} (\tau_e - B \omega_m) \quad (3)$$

Now, transform the above equations into a synchronous reference frame and the electrical dynamics is computed as [6]:

$$D_t^{\alpha_4} \lambda_d = -\frac{R}{L} \lambda_d + \omega_e \lambda_q + \frac{RL_m}{L} i_f \cos \theta \quad (4)$$

$$D_t^{\alpha_5} \lambda_q = -\omega_e \lambda_d - \frac{R}{L} \lambda_q - \frac{RL_m}{L} \lambda_q i_f \sin \theta + V_q \quad (5)$$

$$D_t^{\alpha_6} \theta = \omega_e - \frac{N}{2} \omega_m \quad (6)$$

The output equations are computed as:

$$i_d(t) = \frac{1}{L}\lambda_d - \frac{L_m}{L}i_f \cos \theta \quad (7)$$

$$i_q(t) = \frac{1}{L}\lambda_q + \frac{L_m}{L}i_f \sin \theta \quad (8)$$

Now, equations (4) to (8) are linearized and transformed into fractional order state-space form as:

$$D_t^{\alpha_i} x(t) = Ax(t) + Bu(t) \quad (9)$$

$$y(t) = Cx(t) + Du(t) \quad (10)$$

2.3 Fractional Order Two-Time Scale Modeling of Synchronous Generator

The electrical dynamics of a synchronous generator are fast while mechanical dynamics are slow. The fast and slow states of fractional order two-time scale state-space model of the synchronous generator are given as:

$$x_f(t) = [\lambda_d \quad \lambda_q \quad \theta]^T \quad (11)$$

$$x_s(t) = [\omega_m] \quad (12)$$

These states are associated with slow and fast subsystem equations responsible for the dynamics of synchronous generators.

The input and output vectors are defined as:

$$u(t) = [I_f \quad \omega_e]^T$$

$$y(t) = [I_d \quad I_q]^T$$

If ε is the separation parameter between the fast and slow sub-systems then the fractional order two-time scale state-space model of synchronous generator is given as:

$$\varepsilon D_t^{\alpha_i} x_f(t) = A_{11}x_f(t) + A_{12}x_s(t) + B_1u(t) \quad (13)$$

$$D_t^{\alpha_i} x_s(t) = A_{21}x_f(t) + A_{22}x_s(t) + B_2u(t) \quad (14)$$

$$y(t) = C_1x_f(t) + C_2x_s(t) + Du(t) \quad (15)$$

If the dynamics of the fast system are neglected then the reduced order slow system is derived as:

$$\begin{bmatrix} I_d(s) \\ I_q(s) \end{bmatrix} = \begin{bmatrix} H_{11} & H_{12} \\ H_{21} & H_{22} \end{bmatrix} \begin{bmatrix} I_f(s) \\ W_e(s) \end{bmatrix} \quad (16)$$

If $K_{11}(s)$ and $K_{22}(s)$ are two controllers the closed loop dynamics corresponding to diagonal input-output pairs as reference input signal output pairs then input-output pairs are derive as:

$$\frac{Y_1(s)}{V_1(s)} = G_{11}(s)_{Decoupled} G_{11}(s)_{Coupled} \quad (17)$$

$$\frac{Y_1(s)}{V_2(s)} = G_{12}(s)_{Decoupled} G_{12}(s)_{Coupled} \quad (18)$$

$$\frac{Y_2(s)}{V_1(s)} = G_{21}(s)_{Decoupled} G_{21}(s)_{Coupled} \quad (19)$$

$$\frac{Y_2(s)}{V_2(s)} = G_{22}(s)_{Decoupled} G_{22}(s)_{Coupled} \quad (20)$$

2.4 Hybrid Controller Modeling

Now, in this section, a hybrid control algorithm is developed based on fractional order PID sliding surface and adaptive fuzzy logic using the concept of algorithm developed in [18].

The fractional order PID sliding surfaces for $K_{11}(s)$ and $K_{22}(s)$ controllers are designed as:

$$S_{11} = K_{P_{11}}e_1(t) + K_{I_{11}}D_t^{-\alpha_{11}}e_1(t) + K_{D_{11}}D_t^{\alpha_{11}}e_1(t) \quad (21)$$

$$S_{22} = K_{P_{22}}e_2(t) + K_{I_{22}}D_t^{-\alpha_{22}}e_2(t) + K_{D_{22}}D_t^{\alpha_{22}}e_2(t) \quad (22)$$

The hybrid fractional order sliding mode adaptive fuzzy two-time scale controllers corresponding to these sliding surfaces are designed based on algorithm formulated in [18] as:

$$u_{11}(t) = u_{eq11}^F(t) + K_{SMC_{11}}(D^{\alpha_{11}}e_1(t) + u_{AFLC_{11}}e_1(t) \quad (23)$$

$$u_{22}(t) = u_{eq22}^F(t) + K_{SMC_{22}}(D^{\alpha_{22}}e_2(t) + u_{AFLC_{22}}e_2(t) \quad (24)$$

2.5 Graphical User Interface Development for Model Parameters in LabVIEW

The state space model of the synchronous generator is constructed by inputting model

generator is constructed by inputting model parameters using a graphical user interface (GUI) developed in LabVIEW. The GUI for the design parameters of the synchronous generator is shown in Figure 1 while, the symbolic representation of state space model matrices is shown in Figures 2 and 3.

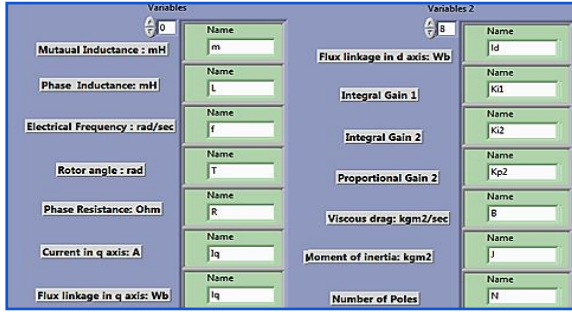


Fig. 1. GUI for design parameters of synchronous generator

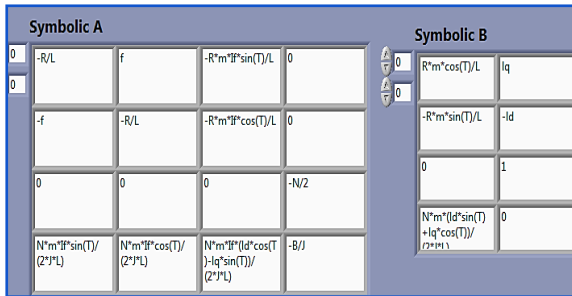


Fig. 2. Symbolic representation of linear model state space matrices A and B

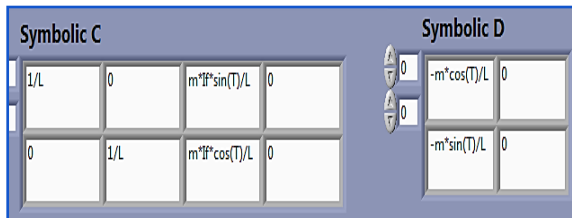


Fig. 3. Symbolic representation of linear model state space matrices C and D

2.6 Synthesis of Reduced Order Synchronous Generator Model

Now, in this section, the reduced order synchronous generator model is developed using equations (9) to (16). The synthesized automated model is developed in LabVIEW as shown in Figures 4 and 5.

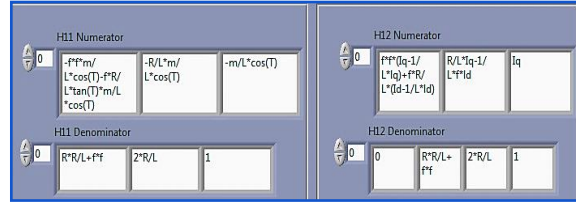


Fig. 4. Symbolic representation of reduced order transfer function elements H_{11} and H_{12}

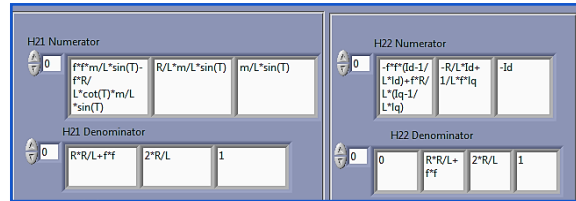


Fig. 5. Symbolic representation of reduced order transfer function elements H_{21} and H_{22}

3. RESULTS AND DISCUSSION

The design, analysis and simulation of synchronous generator is carried out in open loop and closed loop. The design analysis and performance evaluation is carried out in frequency domain and time domain in order to assess the robustness of synthesized model.

3.1. Evaluation of Synthesized Open Loop Framework in Frequency Domain

The reduced order model developed for synchronous generator as shown in Figures 4 and 5 is used for the open loop analysis of transfer function elements in the frequency domain using a Bode plot.

The magnitude and phase plots are designed and analyzed for transfer function elements in LabVIEW as shown in Figures 6 and 7. The frequency response proves that open loop reduced-order dynamics are guaranteed stable as there is not any unstable pole in the transfer functions.

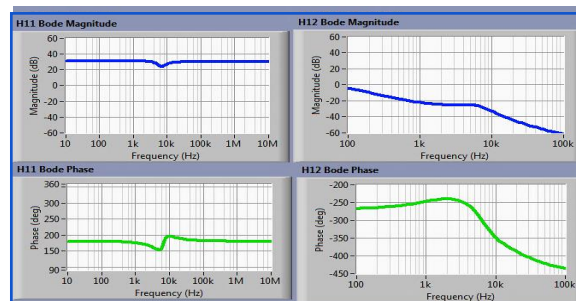


Fig. 6. Open loop frequency response of reduced order system H_{11} and H_{12}

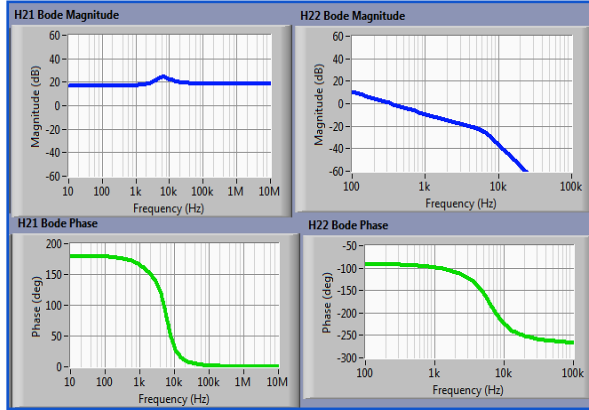


Fig. 7. Open loop frequency response of reduced order system H_{21} and H_{22}

3.2. Evaluation of Synthesized Closed Loop Framework in Frequency Domain

The input-output pairs are configured through a reduced order model with controllers $K_{11}(s)$ and $K_{22}(s)$ as shown in Figure 8. The reduced order model developed for the synchronous generator as shown in Figures 4 and 5 is used for the closed-loop analysis of transfer function elements in the frequency domain using a Bode plot. The magnitude and phase plots are designed and analyzed for transfer function elements in LabVIEW as shown in Figures 9 and 10.

3.3. Evaluation of Synthesized Closed Loop Framework in the Time Domain

The input-output pairs are configured in a closed-loop time domain. The time domain dynamics of internal states are shown in Figure 11. The dynamics of mechanical frequency due to slow and fast subsystems are shown in Figures 12 and 13. Now, the closed-loop dynamics of the full-order system are analyzed and the behaviour of output parameters is shown in Figure 14. The output parameters are

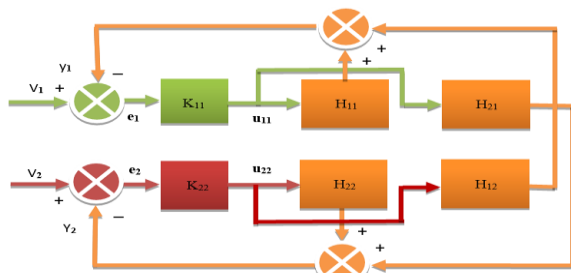


Fig. 8. Closed loop framework of FO-PIDSMC-AFL-TTS control system

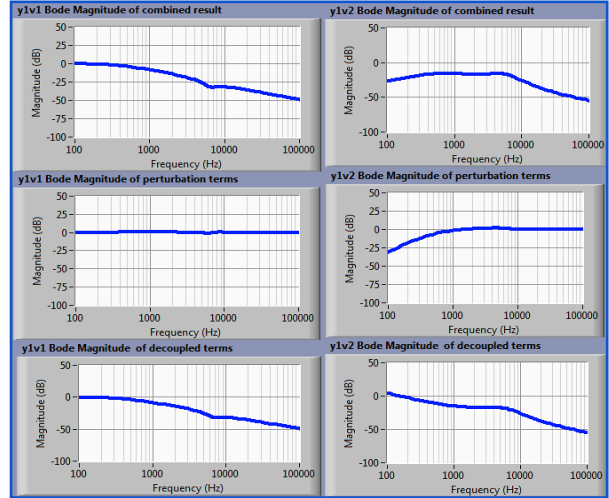


Fig. 9. Closed loop frequency response of decoupled system Y_1V_1 and Y_1V_2

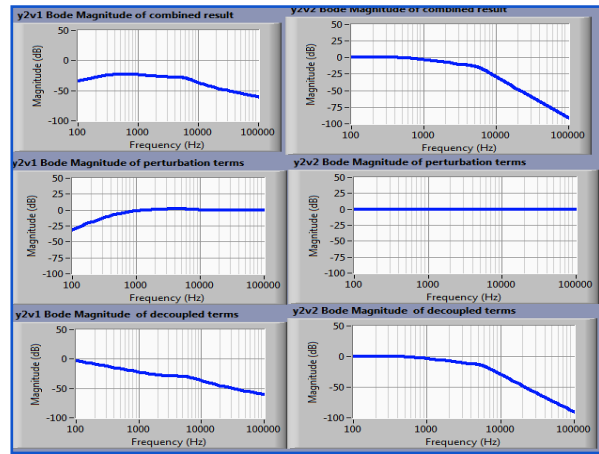


Fig. 10. Closed loop frequency response of decoupled system Y_2V_1 and Y_2V_2

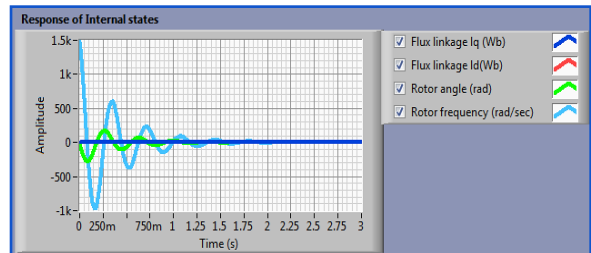


Fig. 11. Time response dynamics of internal states

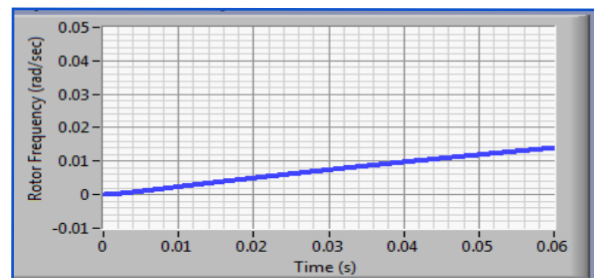


Fig. 12. Time response of mechanical frequency due to slow subsystem

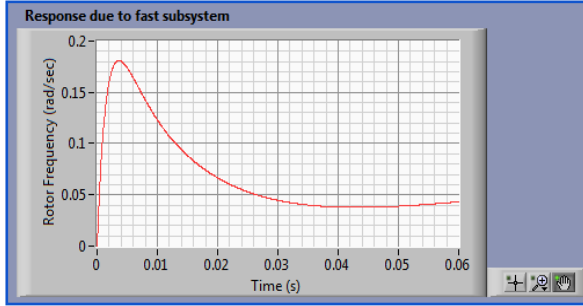


Fig. 13. Time response of mechanical frequency due to fast subsystem

visualized on a per-unit scale.

The inter-comparison of linear, linear fast and nonlinear model responses is assessed in Figure 15 and it is observed that the dynamics of I_d due to the fast system model are fastest and nonlinear and fast linear model dynamics have almost no steady-state error.

The optimized design parameters of model and controllers' framework are obtained using Particle Swam Optimization (PSO) method. The optimized parameters are tabulated in Table 1.

4. CONCLUSION

The synchronous generator is the main electrical equipment on the conventional side of the ACP1000

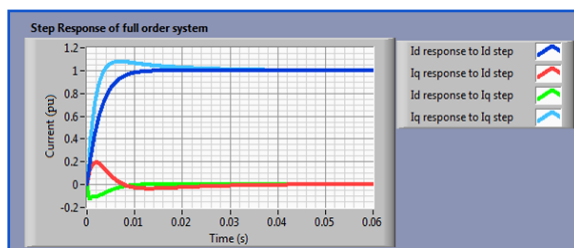


Fig. 14. Closed loop step response of full order feedback model

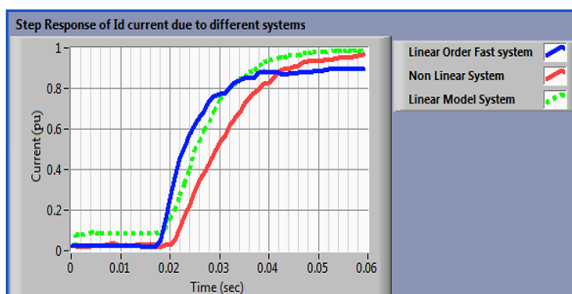


Fig. 15. Closed loop step response comparison of different system models

Table 1. Optimal design parameters of model and controllers

Optimal design parameters	Design values
α_3	0.91
α_4	1.12
α_5	1.22
α_6	0.98
α_{11}	1.40
α_{22}	1.35
K_{SMC11}	1.7
K_{SMC22}	3.4
Number of membership functions for $K_{11}(s)$	14
Number of membership functions for $K_{22}(s)$	18
Scalar design parameters of $K_{11}(s)$	28
Scalar design parameters of $K_{22}(s)$	36

nuclear power plant. A higher order two-time-scale state-space model of synchronous generator is developed in this research work. The stiff two-time-scale model is bifurcated into slow and fast sub-systems. Model reduction is accomplished using a time-scale design philosophy. Two separate controllers are designed for input-output pairs. Controllers are designed using a novel hybrid control design algorithm based on non-linear non-integer sliding mode and intelligent fuzzy logic for a two-time-scale framework in LabVIEW. The design approach is the first step towards two-time-scale and multi-time-scale dynamics of ACP1000 nuclear power plant systems.

5. ACKNOWLEDGEMENTS

The support of the Pakistan Atomic Energy Commission, Chashma Centre of Nuclear Training and Information Support Division of KNP GS is gratefully acknowledged.

6. CONFLICT OF INTEREST

The authors declare no conflict of interest.

7. REFERENCES

1. C. Ernesto, U. Loo, L. Vanfretti, E.L. Castro, and E. Acha. Synchronous generators modeling and control using the framework of individual channel analysis and design. *International Journal of Emerging Electric Power Systems* 08 (05): 1-26 (2007).
2. S. Helmy, A.S. El-Wakeel, M.A. Rahman, and M.A.L. Badr. Real-time modeling and control of

- synchronous generator based on PC. *The Online Journal on Electronics and Electrical Engineering* 10 (07): 1-5 (2009).
3. M. Brazovac, I. Kuzle, and M. Krpan. Detailed mathematical and simulation model of a synchronous generator. *Journal of Energy* 64: 102-129 (2015).
 4. T.S. Daphadar, S.C. Konar, and N.N. Jana. Modelling and control of a 500 MW power system. *International Journal of Advanced Research in Electrical, Electronics and Instrumentation Engineering* 02 (12): 6147-6153 (2013).
 5. A. Fodor, A. Magyar, and K.M. Hangos. Dynamic modeling and model analysis of a large industrial synchronous generator. *International Conference on Applied Electronics, 8-9 September, Pilsen Czech Republic* (2010).
 6. Y.L. Karnavas, and E.I. Lygouras. Synchronous machine analysis and modelling in LabVIEW. *International Journal of Electrical Engineering Education* 0 (0): 1-128 (2018).
 7. M.U. Sardar. Synchronous generator simulation using LabVIEW. *World Academy of Science* 39: 392-400 (2008).
 8. S. Szabo, K.A. Biro, V. Barz, and H.C. Hedesiu. Parameter estimation of synchronous machine by means of LabVIEW environment. *Technical Report of Electrical Machines Department, Technical University of Cluj, Romania* (1998).
 9. G. Dume. Synchronous generator model based on LabVIEW software. *WSEAS Transactions on Advances in Engineering Education* 10 (02): 101-112 (2013).
 10. M.S. Mahmoud. Iterative time-scale separation of synchronous machines. *Applied Math Modeling* 11: 133-140 (1987).
 11. D. Sumina, T. Idzotic, and I. Erceg. Fuzzy logic control of synchronous generator under the condition of transient three phase short circuit. *International power electronics and motion control conference, Portoroz, Slovenia 30 August-01 September*: 1512-1516 (2006).
 12. Y. Chang, and C. Wen. Sliding mode control for synchronous generator. *ISRN Applied Mathematics* 3: 1-7 (2014).
 13. M. Asadollahi, A.R. Ghiasi, and H. Dehghani. Excitation control of a synchronous generator using a novel fractional-order controller. *The Institute of Engineering and Technology Journal* 09 (15): 2255-2260 (2015).
 14. J. Lin, and F.L. Lewis. Two-time scale fuzzy logic controller of flexible link robot arm. *Fuzzy Sets and Systems* 139 (03): 125-149 (2003).
 15. L. Xiong, P. Li, M. Ma, Z. Wang, and J. Wang. Output power quality enhancement of PMSG with fractional order sliding mode control. *Electrical Power and Energy Systems* 115: 105402 (2020).
 16. A.M. Aghazamani, and H. Delavari. Adaptive fractional order sliding mode control for PMSG with disturbance observer. *Tabriz Journal of Electrical Engineering* 50 (03): 1-12 (2022).
 17. A.H. Malik, A.A. Memon, and F. Arshad. Design of fractional order sliding mode adaptive fuzzy switching controllers for uncertain ACP1000 nuclear reactor dynamics. *Proceedings of Pakistan Academy of Sciences-A: Physical and Computational Sciences* 59 (02): 15-28 (2022).